Available online at www.sciencedirect.com
ScienceDirect
Journal of Organometallic Chemistry 691 (2006) 5746–5752
Journal of Organometallic Chemistry
www.elsevier.com/locate/jorganchem

Synthesis of sulfido- and thiolato-bridged Ir_3 cluster and its reactions with alkyne and isocyanide including highly regioselective cyclotrimerization of methyl propiolate

Akihiro Saito, Hidetake Seino, Hidenobu Kajitani, Fusao Takagi, Akihito Yashiro, Takeshi Ohnishi, Yasushi Mizobe *

Institute of Industrial Science, The University of Tokyo, Meguro-ku, Tokyo 153-8505, Japan

Received 22 July 2006; received in revised form 11 September 2006; accepted 14 September 2006
Available online 20 September 2006

Abstract

Reactions of a sulfido- and thiolato-bridged diiridium complex $[(Cp^*Ir)_2(\mu\text{-}S)(\mu\text{-}SCH_2CH_2CN)_2]$ ($Cp^* = \eta^5\text{-}C_5Me_5$) with $[(Cp^*MCl)_2(\mu\text{-}Cl)_2]$ (M = Ir, Rh) afforded the sulfido- and thiolato-bridged trinuclear clusters $[(Cp^*M)(Cp^*Ir)_2(\mu_3\text{-}S)(\mu_2\text{-}SCH_2CH_2CN)_2(\mu_2\text{-}Cl)]Cl$ (**4**: M = Ir, **5**: M = Rh). Upon treatment with XyNC (Xy = 2,6-$Me_2C_6H_3$) in the presence of KPF_6 at 60 °C, **4** was converted into a mixture of a mononuclear XyNC complex $[Cp^*Ir(SCH_2CH_2CN)(CNXy)_2][PF_6]$ (**6**) and a dinuclear XyNC complex $[\{Cp^*Ir(CNXy)\}_2(\mu\text{-}S)(\mu\text{-}SCH_2CH_2CN)][PF_6]$ (**7**). On the other hand, reactions of **4** and **5** with methyl propiolate in the presence of KPF_6 at 60 °C resulted in the formation of a cyclic trimer of the alkyne 1,3,5-$C_6H_3(COOMe)_3$ as the sole detectable organic product. The reactions proceeded catalytically with retention of the cluster cores of **4** and **5**, whereby the activity of the former was much higher than that of the latter.

Keywords: Iridium cluster; Sulfido–thiolato cluster; X-ray structure; Isocyanide complexes; Alkyne cyclotrimerization

1. Introduction

In the course of our studies to develop the intriguing reactivities of the hydrosulfido-bridged multinuclear noble metal complexes [1], we have reported previously the synthesis of $RuIr_2$ sulfido–thiolato clusters $[(Cp^RRu)(Cp^*Ir)_2(\mu_3\text{-}S)(\mu_2\text{-}SCH_2CH_2CN)_2Cl]$ (**1**: $Cp^R = Cp^*$ [2], **2**: $Cp^R = Cp$ [3]; $Cp^* = \eta^5\text{-}C_5Me_5$, $Cp = \eta^5\text{-}C_5H_5$; Chart 1) from the cationic diiridium complex $[(Cp^*Ir)_2(\mu\text{-}SH)_3]Cl$ via $[(Cp^*Ir)_2(\mu\text{-}S)(\mu\text{-}SCH_2CH_2CN)_2]$ (**3**), and demonstrated the reactivities of clusters **1** and **2** toward XyNC (Xy = 2,6-$Me_2C_6H_3$), CO, and alkynes such as HC≡CCOOMe (MP) and MeOCOC≡CCOOMe [2,3].

Now we have found that the related Ir_3 and $RhIr_2$ clusters $[(Cp^*M)(Cp^*Ir)_2(\mu_3\text{-}S)(\mu_2\text{-}SCH_2CH_2CN)_2(\mu_2\text{-}Cl)]Cl$ (**4**: M = Ir, **5**: M = Rh) are also available from **3** and these clusters can catalyze the cyclotrimerization of MP, which presents a striking contrast to the reactions of the $RuIr_2$ clusters **1** and **2** with MP to give an alkyne adduct or a mixture of the uncharacterized MP-containing clusters, respectively. In this paper, we wish to describe the details of synthesis and characterization of **4** and **5** together with their unique reactivities toward MP. The reaction of **4** with XyNC is also reported.

2. Results and discussion

2.1. Synthesis and X-ray structures of 4 and 5

Treatment of **3** with 0.5 equiv. of $[(Cp^*MCl)_2(\mu\text{-}Cl)_2]$ (M = Ir, Rh) in MeCN at room temperature afforded the Ir_3 and Ir_2Rh sulfido–thiolato clusters **4** and **5**, which were isolated as red crystals in 76% and 81% yields, respectively

* Corresponding author. Tel.: +81 3 5452 6360; fax: +81 3 5452 6361.
E-mail address: ymizobe@iis.u-tokyo.ac.jp (Y. Mizobe).

0022-328X/$ - see front matter © 2006 Elsevier B.V. All rights reserved.
doi:10.1016/j.jorganchem.2006.09.017

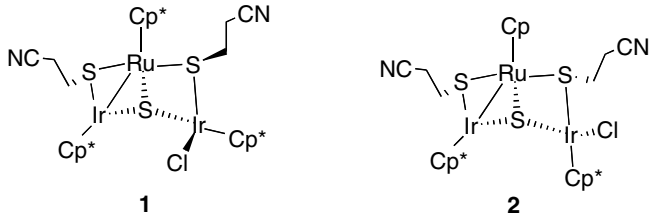

Chart 1.

(Eq. (1)). The structures of **4** and **5** have been determined unambiguously by the X-ray analysis.

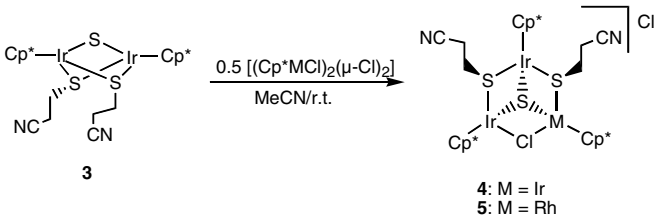

(1)

As shown in Fig. 1, the cation of **4** has an triangular Ir_3 core capped with one almost symmetrically bridging sulfido ligand. The Ir···Ir distances are in the range 3.6460(4)–3.6602(5) Å, indicating the absence of any metal–metal bonding interactions. Two edges of the Ir_3 core are each bridged further by the μ_2-thiolato ligand, the cyanoethyl group of which is oriented toward the direction opposite to the μ_3-S ligand. The remaining Ir···Ir edge is connected by the μ_2-Cl ligand. The Ir–S and Ir–Cl bond lengths and related bond angles in **4** are not exceptional, which are listed in Table 1.

It is noteworthy that in the $RuIr_2$ clusters **1** and **2** the Cl ligand binds to one Ir atom as a terminal ligand and the other Ir center satisfies the 18-electron count by accepting the donation of an electron pair from the Ru atom instead of the Cl ligand. In these clusters, the ^{1}H NMR spectra show two singlets ascribable to the Cp*Ir protons because of the presence of two inequivalent Cp*Ir units. On the other hand, for **4** the protons of the two Cp*Ir fragments connected by the μ_2-Cl ligand are equivalent and observed as one singlet. Thus, the Cp* protons appear as two singlets with the intensities integrated to be 30H and 15H.

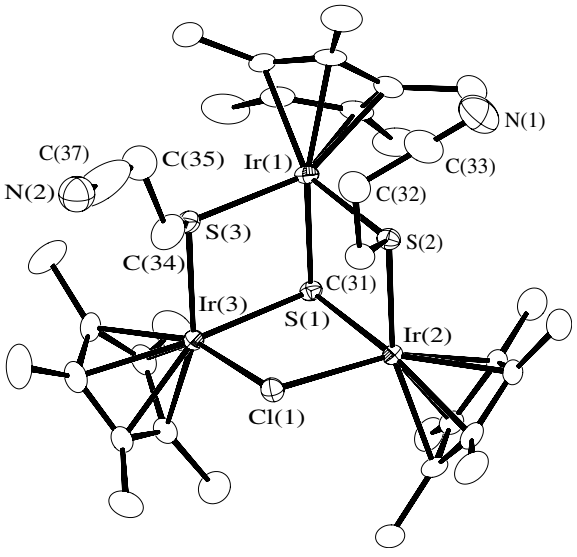

Fig. 1. An ORTEP drawing for the cation in **4** at the 30% probability level. Only one of the two disordered cyanoethyl groups attached to S(3) is shown. Hydrogen atoms are omitted for clarity.

Table 1
Selected bond distances and angles in **4**

Bond distances (Å)			
Ir(1)–S(1)	2.402(2)	Ir(1)–S(2)	2.369(2)
Ir(1)–S(3)	2.371(2)	Ir(2)–S(1)	2.396(2)
Ir(2)–S(2)	2.367(2)	Ir(2)–Cl(1)	2.462(2)
Ir(3)–S(1)	2.397(2)	Ir(3)–S(3)	2.380(2)
Ir(3)–Cl(1)	2.453(2)		
Ir(1)···Ir(2)	3.6460(4)	Ir(1)···Ir(3)	3.6593(3)
Ir(2)···Ir(3)	3.6602(5)		
Bond angles (°)			
S(1)–Ir(1)–S(2)	80.11(6)	S(1)–Ir(1)–S(3)	79.90(7)
S(2)–Ir(1)–S(3)	102.64(7)	S(1)–Ir(2)–S(2)	80.28(7)
S(1)–Ir(2)–Cl(1)	81.28(6)	S(2)–Ir(2)–Cl(1)	91.23(7)
S(1)–Ir(3)–S(3)	79.84(7)	S(1)–Ir(3)–Cl(1)	81.45(6)
S(3)–Ir(3)–Cl(1)	92.73(7)	Ir(1)–S(1)–Ir(2)	98.92(6)
Ir(1)–S(1)–Ir(3)	99.37(8)	Ir(2)–S(1)–Ir(3)	99.59(6)
Ir(1)–S(2)–Ir(2)	100.68(7)	Ir(1)–S(3)–Ir(3)	100.75(9)
Ir(2)–Cl(1)–Ir(3)	96.27(5)		

The structure of **5** is essentially the same as that of **4**, except that the position of either Ir(2) or Ir(3) in **4** is occupied by Rh; viz., in the crystal, the Rh atom is disordered over these two positions with the occupancies of 0.5 and 0.5. Observed metal–metal separations (Ir(1)···M(2), 3.6327(5); Ir(1)···M(3), 3.6456(4); M(2)···M(3), 3.6180(6) Å) are slightly shorter than those in **4**. Due to the incorporation of Rh into one of these two sites, three Cp* groups become mutually inequivalent and the ^{1}H NMR spectrum of **5** exhibits three singlets with the same intensities assignable to the Cp* protons.

2.2. Reactions of 4 with XyNC

Reactivities of the new cluster **4** toward XyNC and MP have been investigated for comparison with those of **1** and **2**. As reported previously [2,3], when **1** and **2** are treated with one or more equivalents of XyNC at room temperature in the presence of KPF_6, the Cl ligand bound to Ir is replaced by XyNC to give mono XyNC clusters $[(Cp^RRu)(Cp^*Ir)_2(\mu_3\text{-}S)(\mu_2SCH_2CH_2CN)_2(CNXy)][PF_6]$. In contrast, treatment of **4** with 1 equiv. of XyNC in MeCN at 60 °C in the presence of KPF_6 afforded the mixture containing two XyNC complexes and unreacted **4**. At room temperature, reaction did not occur. Attempts have been made to optimize the yields of these two XyNC complexes, and we have found that when treated with 4.4 equiv. of XyNC and 3.4 equiv. of KPF_6 in MeCN at 60 °C, **4** is converted cleanly to a 1:1 mixture of the Ir complexes to be characterized as a mononuclear complex $[Cp^*Ir(SCH_2CH_2CN)(CNXy)_2][PF_6]$ (**6**) and a dinuclear complex $[\{Cp^*Ir(CNXy)\}_2(\mu\text{-}S)(\mu\text{-}SCH_2CH_2CN)][PF_6]$ (**7**) generated through

degradation of the trinuclear core of **4**. The isolated yields of **6** and **7** were 43% and 74%, respectively, based on the stoichiometry shown in Eq. (2)

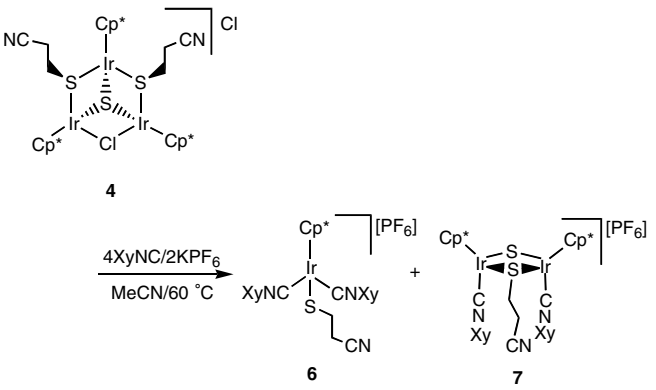

(2)

The structures of **6** and **7** have been determined by the single-crystal X-ray analysis. Complex **6** has a three-legged piano stool structure as shown in Fig. 2. Selected metrical parameters are listed in Table 2. Two isocyanide molecules are bonded to the Ir center in an end-on manner with essentially linear Ir–C–N–C arrays (Ir–C–N angles: 179.1(4) and 179.4(5)°, C–N–C angles: 175.3(6) and 175.6(7)°). This feature is consistent with the observed short isocyano C–N bond distances at 1.146(7) and 1.160(8) Å and the appearance of two strong ν(N≡C) bands at 2186 and 2155 cm^{-1} due to the XyNC ligands in the N–C triple bond region in its IR spectrum. The Cp^*Ir XyNC complexes with sulfur coligands are not precedented except for the clusters $[(Cp^RRu)(Cp^*Ir)_2(\mu_3\text{-}S)(\mu_2\text{-}SCH_2CH_2CN)_2(CNXy)][PF_6]$ described in the previous papers, for which the ν(N≡C) bands are observed at 2114 cm^{-1} ($Cp^R = Cp^*$) [2] and 2125 cm^{-1} ($Cp^R = Cp$) [3], respectively. For comparison, those of the Cp^*Ir^{III} complexes $[Cp^*IrI_2(CNXy)]$ [4], $[Cp^*IrCl\{PPh_2(C_6H_3(OMe)_2)\}(CNXy)][PF_6]$ [5], and $[\{Cp^*IrCl(CNXy)\}_2(\mu\text{-}Ph_2PC_{10}H_6PPh_2)][OSO_2CF_3]_2$ [6] are 2140, 2160, and 2155 cm^{-1}.

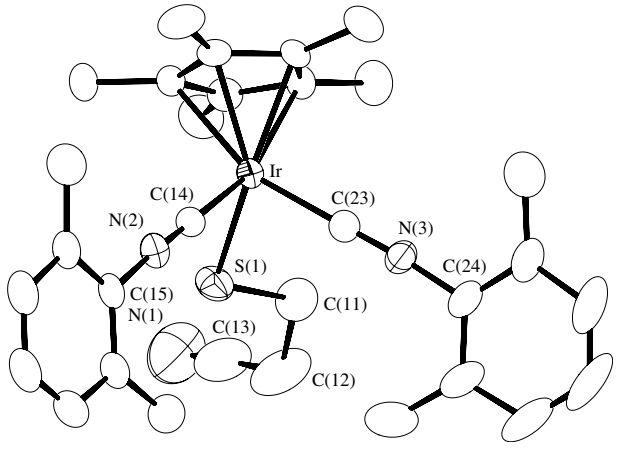

Fig. 2. An ORTEP drawing for the cation in **6** at the 30% probability level. Hydrogen atoms are omitted for clarity.

Table 2
Selected bond distances and angles in **6**

Bond distances (Å)			
Ir–S(1)	2.388(2)	Ir–C(14)	1.952(5)
Ir–C(23)	1.941(6)	C(14)–N(2)	1.146(7)
C(23)–N(3)	1.160(8)	N(2)–C(15)	1.396(7)
N(3)–C(24)	1.392(8)		
Bond angles (°)			
S(1)–Ir–C(14)	84.9(2)	S(1)–Ir–C(23)	89.2(2)
C(14)–Ir–C(23)	91.0(2)	Ir–C(14)–N(2)	179.1(4)
Ir–C(23)–N(3)	179.4(5)	C(14)–N(2)–C(15)	175.3(6)
C(23)–N(3)–C(24)	175.6(7)		

Fig. 3 shows the structure of **7** having the dinuclear core bridged by the sulfido and thiolato ligands. Although the single crystal contains two crystallographically independent molecules of **7**, the structures of these two are essentially the same and only one is depicted. Important interatomic distances and angles for two molecules are summarized in Table 3. In **7**, two Ir centers without any direct Ir–Ir bonding interactions (Ir···Ir distances: 3.6454(4) and 3.6471(4) Å) are connected by one sulfide and one thiolate, whereby the four-membered Ir_2S_2 ring is folded slightly with the dihedral angles along the S–S vector of 171° and 170° for molecules 1 and 2, respectively. Two Cp^* ligands are mutually syn with respect to this Ir_2S_2 ring and the cyanoethyl group in the thiolato ligand is oriented to the direction opposite to the Cp^* ligands.

As for the linkages around S atoms, the Ir–S bonds associated with the sulfido ligands Ir(1)–S(1) and Ir(2)–S(1) (2.388(2)–2.393(2) Å) are somewhat longer than those for the thiolato ligands Ir(1)–S(2) and Ir(2)–S(2) (2.345(2)–2.361(2) Å), where the Ir–S–Ir angles are 99.37(8)° and 99.33(7)° for S(1) and 101.77(8)° and 101.40(7)° for S(2). On the other hand, for the triply bridged sulfido–thiolato complex **3** with a Ir···Ir distance at 3.324(1) Å, both the

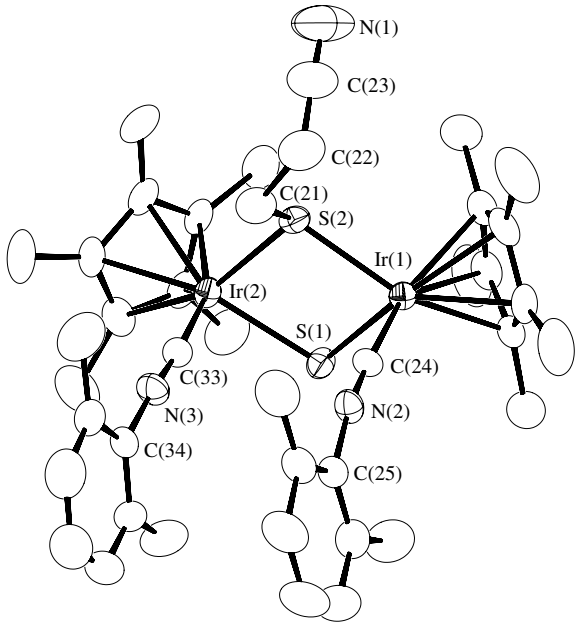

Fig. 3. An ORTEP drawing for the cation in **7** at the 30% probability level. Hydrogen atoms are omitted for clarity.

Table 3
Selected bond distances and angles in **7**

	Molecule 1	Molecule 2
Bond distances (Å)		
Ir(1)–S(1)	2.393(2)	2.393(2)
Ir(1)–S(2)	2.353(2)	2.352(2)
Ir(2)–S(1)	2.388(2)	2.392(2)
Ir(2)–S(2)	2.345(2)	2.361(2)
Ir(1)–C(24)	1.893(7)	1.920(8)
Ir(2)–C(33)	1.893(8)	1.915(9)
C(24)–N(2)	1.169(9)	1.13(1)
C(33)–N(3)	1.18(1)	1.13(1)
N(2)–C(25)	1.41(1)	1.41(1)
N(3)–C(34)	1.40(1)	1.42(1)
Ir(1)···Ir(2)	3.6454(4)	3.6471(4)
Bond angles (°)		
S(1)–Ir(1)–S(2)	78.83(7)	79.14(7)
S(1)–Ir(1)–C(24)	85.1(3)	89.0(2)
S(2)–Ir(1)–C(24)	95.6(2)	95.6(3)
S(1)–Ir(2)–S(2)	79.11(7)	78.99(7)
S(1)–Ir(2)–C(33)	91.6(2)	89.7(3)
S(2)–Ir(2)–C(33)	96.2(3)	94.2(3)
Ir(1)–S(1)–Ir(2)	99.37(8)	99.33(7)
Ir(1)–S(2)–Ir(2)	101.77(8)	101.40(7)
Ir(1)–C(24)–N(2)	176.3(7)	173.6(8)
Ir(2)–C(33)–N(3)	174.7(8)	174.9(8)
C(24)–N(2)–C(25)	165.4(9)	174.0(9)
C(33)–N(3)–C(34)	170.9(9)	173.5(9)

bond lengths and bond angles associated with the sulfido S atom (Ir–S: 2.388(3), 2.384(2) Å; Ir–S–Ir: 88.28(8)°) are essentially identical to those associated with the thiolato S atoms (Ir–S: 2.382(2)–2.395(2) Å; Ir–S–Ir: 87.90(7)°, 88.36(8)°) [7]. For comparison, the doubly bridged thiolato complex $[(Cp^*IrCl)_2(\mu\text{-}SPr^i)_2]$ has a slightly puckered Ir_2S_2 core with the dihedral angle along the S–S vector of 173° and the Ir···Ir distance at 3.665(2) Å, for which the Ir–S bond lengths are 2.391(2) and 2.400(2) Å and the Ir–S–Ir angle is 99.82(8)°, respectively [8]. In the doubly bridged sulfido complex $[\{Cp^*Ir(CNBu^t)\}_2(\mu\text{-}S)_2]$ having a planar Ir_2S_2 core with two mutually *trans* isocyanide ligands, the Ir–S bond lengths are 2.367(2) and 2.376(3) Å, while the Ir–S–Ir angle is 100.68(9)° [9]. In **7**, two isocyanide ligands are coordinating in an end-on fashion as observed in **6**, where two Xy groups are situated in parallel to each other. The IR and ^{1}H NMR spectra are consistent with the solid state structure clarified by the X-ray analysis.

2.3. Reactions of *4* with MP

In the previous paper [2], we reported that the reaction of **1** with MP in the presence of KPF_6 at room temperature resulted in the incorporation of one alkyne molecule as an μ_2-bridge between two Ir centers to give the fully characterized cluster $[(Cp^*Ru)(Cp^*Ir)_2(\mu_3\text{-}S)(\mu_2SCH_2CH_2CN)_2(\mu_2\text{-}HC{\equiv}CCOOMe)][PF_6]$ (**8**; Chart 2). On the other hand, analogous treatment of the CpRu cluster **2** did not proceed cleanly and gave the mixture of the clusters that are not fully characterized, although the spectral data of one product strongly suggested its structure to be analogous to **8**.

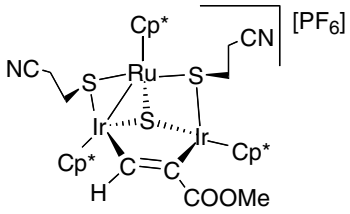

8

Chart 2.

Now, we have found that when **4** is treated with 4 equiv. of MP in the presence of KPF_6 at 60 °C in MeCN for 12 h, the cyclic trimer 1,3,5-$C_6H_3(COOMe)_3$ (**9**) was obtained as the sole product in the yield of 0.99 mol/mol **4**. Cluster **4** was recovered almost quantitatively.

Based on this finding, further study has been carried out to clarify the activity of **4** toward the catalytic cyclotrimerization of MP, and this has revealed that the reaction of MP in the presence of ca. 1 mol% **4** and ca. 4 mol% KPF_6 in MeCN at 60 °C afforded **9** in 84% yield (TON = 32) after 69 h (Eq. (3)). The ^{1}H NMR spectrum of the reaction mixture showed the absence of any other organic products than **9**, together with the presence of only **4** as the Ir-containing compounds in product solution. It is to be noted that the Ir_2Rh cluster **5** also catalyzes the formation of **9** under the similar conditions but the activity is much lower; the yield of **9** after 72 h was 11% (TON = 3.6). As for the solvent, the reaction also proceeded in DMF, whereas those in dichloroethane and alcohols such as EtOH and MeOH were quite slow. With respect to the alkyne, non-activated alkynes, e.g. 1-octyne and phenylacetylene, did not react under these conditions

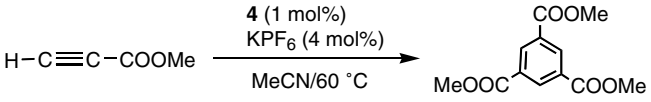

9

(3)

Catalytic [2 + 2 + 2] cyclotrimerization of alkynes is attracting much attention as the convenient methods to prepare substituted benzenes. Extensive studies have already disclosed that many transition metal complexes containing Co, Rh, Ru, Pt, Mo, Ta, Ti, etc., can catalyze the reactions of this type [10]. Certain Ir complexes are also known to promote alkyne cyclotrimerization [11] but the precedented examples are still limited. Furthermore, well-defined systems that involve the multinuclear complexes as active species are rare. It is also to be noted that it is generally difficult to attain the high regioselectivity for the intermolecular cyclotrimerization of terminal alkynes. Highly selective formation of **9** by the use of the Ir cluster **4** observed in this study is therefore quite interesting.

Since no intermediate stages were isolated or detected even under controlled reaction conditions, the mechanism operating in the present system is uncertain. However,

previous findings that the reactions of **1** and **2** with MP afford the clusters consisting of MP bridging between two Ir atoms may suggest that this trimerization using **4** probably proceeds via the initial formation of the analogous alkyne adduct, followed by the successive insertion of two MP molecules into the Ir–C bonds. Exceptionally, high regioselectivity favoring 1,3,5-substituted trimer observed for this system might be ascribable to this mechanism featuring the bimetallic site. Indeed, treatment of the MP adduct **8** with 100 equiv. of MP in MeCN at 60 °C resulted in the formation of the trimer **9** with retention of the cluster cores of all **8**, although the yield was low (TON = 1.3 after 24 h).

In contrast, other cyclotrimerization reactions catalyzed by numerous transition metal complexes generally proceed via the mechanism involving the mononuclear metallacyclopentadiene complexes as key intermediate stages, which tend to result in the formation of a mixture of 1,3,5- and 1,2,4-substituted trimers from terminal alkynes with the latter predominant [10]. Significant difference in the catalytic activity between the Ir_3 cluster **4** and the Ir_2Rh cluster **5** indicates that the Rh center is involved in the active site of the latter, which might also support indirectly this dinuclear mechanism.

3. Experimental

3.1. General

All manipulations were carried out under N_2 using standard Schlenk techniques. Solvents were dried by common methods and distilled under N_2 before use. Complex **3**, $[(Cp^*MCl)_2(\mu\text{-}Cl)_2]$ (M = Ir, Rh) were prepared according to the literature methods [12], while other chemicals used in this study were obtained commercially and used as received.

NMR and IR spectra were measured on a JEOL alpha-400 or a JASCO FT/IR-420 spectrometer at room temperature. Characterization of organic compounds by GC–MS methods was carried out using a Shimadzu GC–MS QP-5050 spectrometer, and determination of their quantities by GLC methods was on a Shimadzu GC-14B gas chromatograph equipped with a 25 m × 0.25 mm CBP 10 fused silica capillary column. Elemental analyses were done with a Perkin–Elmer 2400 series II CHN analyzer.

3.2. Preparation of 4

Into a MeCN solution (150 cm^3) of **3** (1.29 g, 1.50 mmol) was added $[(Cp^*IrCl)_2(\mu\text{-}Cl)_2]$ (598 mg, 0.751 mmol), and the mixture was stirred at room temperature for 20 h. The resultant mixture was dried up in vacuo and the residue was washed with ether. Crystallization of the remained solid from MeCN–ether afforded **4** · 1.75MeCN as red crystals (1.51 g, 76%). Anal. Calc. for $C_{39.5}H_{58.25}N_{3.75}S_3Cl_2Ir_3$ requires C, 35.69; H, 4.42; N, 3.95. Found: C, 35.47; H, 4.44; N, 4.06%. ^1H NMR (δ, CD_3CN): 1.55 (s, 30H, Cp^*), 1.59 (s, 15H, Cp^*), 2.46 (t, $J = 8$ Hz, 4H, CH_2), 2.77–2.84 (m, 2H, CH_2), 3.01–3.08 (m, 2H, CH_2). IR (KBr, cm^{-1}): 2244 (C≡N).

3.3. Preparation of 5

This compound was prepared similarly from **3** (43 mg, 0.050 mmol) and $[(Cp^*RhCl)(\mu\text{-}Cl)_2]$ (16 mg, 0.025 mmol) as red crystals (48 mg, 81% yield). *Anal.* Calc. for $C_{36}H_{53}N_2S_3Cl_2Ir_2Rh$ requires C, 37.01; H, 4.57; N, 2.40. Found: C, 36.55; H, 4.66; N, 2.72%. ^1H NMR (δ, CD_3CN): 1.51, 1.57, 1.62 (s, 15H each, Cp^*), 2.40–2.44 (m, 2H, CH_2), 2.48 (t, $J = 8$ Hz, 2H, CH_2), 2.67–2.78 (m, 2H, CH_2), 2.93–3.05 (m, 2H, CH_2). IR (KBr, cm^{-1}): 2245 (C≡N). A single crystal of **5** used for the X-ray analysis was sealed in a glass capillary without drying, which contained two solvating acetonitrile molecules per one cluster molecule.

3.4. Reaction of 4 with XyNC to give 6 and 7

Complex **4** · 1.75MeCN (67 mg, 0.050 mmol), XyNC (29 mg, 0.22 mmol), and KPF_6 (31 mg, 0.17 mmol) were added into MeCN (5 cm^3) and the mixture was stirred for 31 h at 60 °C. The resultant mixture was filtered and ether was added to the concentrated filtrate, affording a 2:3 mixture of **6** and **7** as orange microcrystals (55 mg) together with small amounts of pure **6** · 0.5Et_2O as pale-yellow crystals (1 mg) and **7** as red crystals (6 mg) that are separable manually. Additional amounts of pure crystals of **6** and **7** were obtained by recrystallizing the microcrystalline mixture of these two. **6** · 0.5Et_2O: 43% yield. *Anal.* Calc. for $C_{33}H_{42}N_3O_{0.5}F_6PSIr$ requires C, 46.20; H, 4.93; N, 4.90. Found: C, 46.25; H, 4.51; N, 4.79%. ^1H NMR (δ, CD_3CN): 2.14 (s, 15H, Cp^*), 2.43 (s, 12H, Me in Xy), 2.55, 2.72 (t, $J = 6.9$ Hz, 2H each, CH_2), 7.20–7.35 (m, 6H, C_6H_3). IR (KBr, cm^{-1}): 2249w ($CH_2C{\equiv}N$), 2186s, 2155s (XyN≡C). **7**: 74% yield. *Anal.* Calc. for $C_{41}H_{52}N_3F_6PS_2Ir_2$ requires C, 41.72; H, 4.44; N, 3.56. Found: C, 41.83; H, 4.33; N, 3.84%. ^1H NMR (δ, CD_3CN): 1.84 (s, 30H, Cp^*), 2.26 (s, 12H, Me in Xy), 2.38, 2.84 (t, $J = 7.5$ Hz, 2H each, CH_2), 6.80–6.95 (m, 6H, C_6H_3). IR (KBr, cm^{-1}): 2252w ($CH_2C{\equiv}N$), 2131s (XyN≡C).

3.5. Reactions of 4 with MP

(1) A mixture of **4** · 1.75MeCN (67 mg, 0.050 mmol), KPF_6 (28 mg, 0.15 mmol), and MP (17 mg, 0.20 mmol) in MeCN (5 cm^3) was stirred at 60 °C for 12 h. The ^1H NMR spectrum of the product mixture containing Ph_3CH (25 mg) as an internal standard showed that the yield of **9** was 0.99 mol/mol **4** charged, while **4** present in the product solution was 92% of the amount initially charged. From the ^1H NMR criteria, the trimer **9** was the sole organic product and the cluster **4** was the only detectable Ir-containing compound.

(2) As for the typical catalytic reaction, a mixture of **4** · 1.75MeCN (15 mg, 0.011 mmol), KPF_6 (7 mg, 0.05 mmol), and MP (108 mg, 1.28 mmol) in MeCN

Table 4
Crystallographic data for **4** · 1.75MeCN, **5** · 2MeCN, **6** · 0.5Et_2O, and **7**

	4 · 1.75MeCN	**5** · 2MeCN	**6** · 0.5Et_2O	**7**
Formula	$C_{39.5}H_{58.25}Cl_2Ir_3N_{3.\ 75}S_3$	$C_{40}H_{59}Cl_2N_4S_3Rh$	$C_{33}H_{42}F_6IrN_3O_{0.5}PS$	$C_{41}H_{52}F_6Ir_2N_3PS_2$
Formula weight	1329.42	1250.36	857.96	1180.41
Space group	$P\bar{1}$ (no. 2)	$P\bar{1}$ (no. 2)	$P\bar{1}$ (no. 2)	$P\bar{1}$ (no. 2)
Unit cell dimensions				
a (Å)	12.535(5)	12.515(1)	8.662(2)	13.224(2)
b (Å)	12.689(5)	12.690(2)	11.774(3)	14.666(2)
c (Å)	15.726(6)	15.619(2)	18.877(5)	24.185(4)
α (°)	68.65(1)	68.73(1)	78.635(8)	91.847(2)
β (°)	77.71(1)	77.620(9)	82.174(8)	103.352(3)
γ (°)	82.02(1)	82.09(1)	76.089(8)	90.232(2)
V (Å^3)	2271(2)	2252.9(5)	1824.0(8)	4561(1)
Z	2	2	2	4
ρ_{calc} (g cm^{-3})	1.944	1.843	1.562	1.719
μ_{calc} (cm^{-1})	90.79	65.60	38.29	60.28
Crystal size (mm^3)	0.40 × 0.40 × 0.20	0.60 × 0.40 × 0.30	0.60 × 0.40 × 0.30	0.30 × 0.30 × 0.20
Number of unique data	10613	8224	8537	21410
Number of observed data	9722 ($I > 2\sigma(I)$)	7109 ($I > 2\sigma(I)$)	7091 ($I > 2\sigma(I)$)	13252 ($I > 2\sigma(I)$)
Transmission factor	0.036–0.163	0.091–0.140	0.234–0.317	0.207–0.300
R_1[a]	0.050	0.037	0.039	0.042
wR_2[b]	0.132	0.096	0.114	0.133
GOF[c]	1.037	1.006	1.041	1.014
Residual peaks (e$^-$ Å^{-3})	4.74, −2.33	1.53, −1.29	2.49, −1.43	2.54, −2.68

[a] $R_1 = \sum\|F_o| - |F_c\|/\sum|F_o|$ (observed data).
[b] $wR_2 = [\sum(wF_o^2F_c^2)/\sum w(F_o^2)^2]^{1/2}$ (all data).
[c] GOF $= [\sum w(|F_o| - |F_c|)^2/\{$(no. observed) − (no. variables)$\}]^{1/2}$.

(5 cm^3) was stirred at 60 °C. Conversion of MP was monitored by GLC analysis of the reaction mixtures after adding toluene as an internal standard. After all MP was consumed, the yield of **9** was determined by the ^{1}H NMR spectrum. Other catalytic reactions were also carried out in the analogous manner.

3.6. X-ray crystallography

Single crystals of **4** · 1.75MeCN, **5** · 2MeCN, **6** · 0.5Et_2O, and **7** were sealed in glass capillaries under argon and mounted on a Rigaku Mercury-CCD (for **4**, **6**, and **7**) or AFC7R (for **5**) diffractometer equipped with a graphite-monochromatized Mo Kα source. All diffraction studies were done at 23 °C, the details of which are listed in Table 4.

Structure solution and refinements were carried out by using the CRYSTALSTRUCTURE program package [13]. The position of the non-hydrogen atoms were determined by Patterson methods (PATTY) [14] and subsequent Fourier synthesis (DIRDIF 99) [15]. These were refined with anisotropic thermal parameters by full-matrix least-squares techniques. For **4**, the β-C and N atoms in the cyanoethyl group attached to S(3) are disordered over two positions with the occupancies of 0.65 and 0.35 and these were refined isotropically with the restraint of the C–N bond distance at 1.2 Å for the C and N atoms with less occupancy. Restraints were also employed for the C–C and C–N bond distances in the solvating MeCN molecule with occupancy at 1.0 at 1.6 and 1.2 Å, respectively. For **5**, the Rh atom is disordered over two positions, which were refined as the 1:1 mixtures of Rh and Ir. The β-C atom as well as the cyano C and N atoms in the cyanoethyl group on S(3) were disordered over two positions in a ratio 0.5:0.5, which were refined isotropically. For **6**, a solvating Et_2O molecule with a occupancy of 0.5 was located near the center of symmetry, which was modeled with restraints of bond distances and angles and these five atoms were refined isotropically with the same thermal parameters. For **7**, two crystallographically independent molecules were found in the asymmetric unit. Six F atoms of one of the two PF_6 anions were each disordered in two orientations in a ratio of 0.6:0.4. Hydrogen atoms except for those of the disordered cyanoethyl group in **4** and **5** together with those of the solvating Et_2O for **6** · 0.5Et_2O were placed at the calculated positions and included in the refinements with fixed parameters.

Supplementary material

CCDC 615217, 615218, 615219 and 615220 contain the supplementary crystallographic data for **4**, **5**, **6** and **7**. These data can be obtained free of charge via http://www.ccdc.cam.ac.uk/conts/retrieving.html, or from the Cambridge Crystallographic Data Centre, 12 Union Road, Cambridge CB2 1EZ, UK; fax: (+44) 1223-336-033; or e-mail: deposit@ccdc.cam.ac.uk.

Acknowledgements

This work was supported by a Grant-in-Aid for Scientific Research on Priority Areas (No. 14078206, "Reaction

Control of Dynamic Complexes'') from the Ministry of Education, Culture, Sports, Science and Technology, Japan, and by CREST of JST (Japan Science and Technology Agency).

References

[1] (a) See for example: M. Hidai, Y. Mizobe, Can. J. Chem. 83 (2005) 358;
(b) M. Hidai, S. Kuwata, Y. Mizobe, Acc. Chem. Res. 33 (2000) 46;
(c) Z. Tang, Y. Nomura, S. Kuwata, Y. Ishii, Y. Mizobe, M. Hidai, Inorg. Chem. 37 (1998) 4909;
(d) W.-Y. Yeh, H. Seino, T. Amitsuka, S. Ohba, M. Hidai, Y. Mizobe, J. Organomet. Chem. 689 (2004) 2338.
[2] F. Takagi, H. Seino, M. Hidai, Y. Mizobe, Organometallics 22 (2003) 1065.
[3] H. Kajitani, H. Seino, Y. Mizobe, Organometallics 24 (2005) 6260.
[4] W.D. Jones, R.P. Duttweiler Jr., F.J. Feher, Inorg. Chem. 29 (1990) 1505.
[5] Y. Yamamoto, K. Kawasaki, S. Nishimura, J. Organomet. Chem. 587 (1999) 49.
[6] Y. Yamamoto, F. Miyauchi, Inorg. Chim. Acta 334 (2002) 77.
[7] F. Takagi, H. Seino, M. Hidai, Y. Mizobe, J. Chem. Soc., Dalton Trans. (2002) 3603.
[8] M. Nishio, H. Matsuzaka, Y. Mizobe, M. Hidai, Inorg. Chim. Acta 263 (1997) 119.
[9] D.A. Dobbs, R.G. Bergman, Inorg. Chem. 33 (1994) 5329.
[10] (a) S. Saito, Y. Yamamoto, Chem. Rev. 100 (2000) 2901;
(b) N.E. Schore, Chem. Rev. 88 (1988) 1081;
(c) D.B. Grotjahn, in: E.W. Abel, F.G.A. Stone, G. Wilkinson, L.S. Hegedus (Eds.), Comprehensive Organometallic Chemistry II, vol. 12, Pergamon, Oxford, 1995 (Chapter 7.3);
(d) R. Schmid, K. Kirchner, Eur. J. Inorg. Chem. (2004) 2609.
[11] (a) M. Fabbian, N. Marsich, E. Farnetti, Inorg. Chim. Acta 357 (2004) 2881;
(b) E. Farnetti, N. Marsich, J. Organomet. Chem. 689 (2004) 14;
(c) C. Bianchini, K.G. Caulton, C. Chardon, M.-L. Doublet, O. Eisenstein, S.A. Jackson, T.J. Johnson, A. Meli, M. Peruzzini, W.E. Streib, A. Vacca, F. Vizza, Organometallics 13 (1994) 2010.
[12] R.N. Grimes, Inorg. Synth. 29 (1992) 229.
[13] D.J. Watkin, C.K. Prout, J.R. Carruthers, P.W. Betteridge, CRYSTALS Issue 10, CRYSTALSTRUCTURE 3.6.0: Crystal Structure Analysis Package, Rigaku and Rigaku/MSC, 2000–2004, 9009 New Trails Dr., The Woodlands, TX, USA.
[14] P.T. Beurskens, G.Admiraal, G. Beurskens, W.P. Bosman, S. Garcia-Granda, R.O. Gould, J.M.M. Smits, C. Smykall, PATTY, The DIRDIF program system; Technical Report of the Crystallography Laboratory, University of Nijmegen, Nijmegen, The Netherlands, 1992.
[15] P.T. Beurskens, G.Admiraal, G. Beurskens, W.P. Bosman, R. de Gelder, R. Israel, J.M.M. Smits, DIRDIF99, The DIRDIF 99 Program System, Technical Report of the Crystallography Laboratory, University of Nijmegen, Nijmegen, The Netherlands, 1999.